

Scaling properties of inclusive W^\pm production at hadron colliders

François Arleo,^a Émilien Chapon,^a Hannu Paukkunen^{b,c}

^a*Laboratoire Leprince-Ringuet (LLR), École polytechnique, CNRS/IN2P3 91128 Palaiseau, France*

^b*Department of Physics, University of Jyväskylä, P.O. Box 35, FI-40014 University of Jyväskylä, Finland*

^c*Helsinki Institute of Physics, P.O. Box 64, FI-00014 University of Helsinki, Finland*

E-mail: francois.arleo@cern.ch, emilien.chapon@cern.ch,
hannu.paukkunen@jyu.fi

ABSTRACT: We consider the hadroproduction of W gauge bosons in their leptonic decay mode. Starting from the leading-order expressions, we show that by defining a suitable scaling variable the center-of-mass dependence of the cross sections at the LHC energies can be essentially described by a simple power law. The scaling exponent is directly linked to the small- x behaviour of quark distributions which, at the high virtualities involved in W production, is largely dictated by QCD parton evolution. This entails a particularly simple scaling law for the lepton charge asymmetry and also predicts that measurements in different collision systems (p-p, p- \bar{p} , p-Pb Pb-Pb) are straightforwardly related. The expectations are compared with the existing data and a very good overall agreement is observed. A precision observable that can be measured at the LHC is proposed.

KEYWORDS: W boson, QCD, hadronic colliders, parton distribution functions

Contents

1	Introduction	1
2	Derivation of the scaling properties	2
2.1	Absolute cross sections	2
2.2	Charge asymmetries	4
3	Scaling vs. NLO calculation	5
4	Data and predictions	8
4.1	Comparison with existing data	8
4.2	Predictions	13
5	Summary	15

1 Introduction

The production of W gauge bosons in hadronic collisions is a process which is sensitive to practically all aspects of Standard Model, from electro-weak couplings to QCD dynamics and the non-perturbative parton content of the hadrons. One of the most precisely measured observables at hadron colliders is the rapidity (y) dependence of the lepton charge asymmetry, \mathcal{C}_ℓ ,

$$\mathcal{C}_\ell(y) \equiv \frac{d\sigma^{\ell^+}/dy - d\sigma^{\ell^-}/dy}{d\sigma^{\ell^+}/dy + d\sigma^{\ell^-}/dy}, \quad (1.1)$$

where the charged lepton ($\ell = e, \mu$) originates from the leptonic decay of the W boson. This observable is a useful probe of proton parton distribution functions (PDFs), in particular, to disentangle the flavour dependence [1, 2] which is not well constrained by the deep inelastic scattering.¹ Today, the charge asymmetry has been studied in detail by the CDF [3, 4] and D0 [5–8] experiments in p– \bar{p} collisions at the Tevatron as well as the ATLAS [9, 10], CMS [11, 12], and LHCb [13] experiments in p–p collisions at the LHC. While the broad features of the experimental data are well captured by fixed-order perturbative QCD calculations [14, 15], the simultaneous reproduction of the D0 data in bins of different kinematic cuts is known to pose difficulties [16, 17].

The first measurements of W production in p–Pb collisions have recently appeared [18, 19] and various observables seem to favour the use of EPS09 nuclear PDFs (nPDFs) [20] instead of a naive superposition of free nucleon PDFs (similar conclusion can be expected in the case of other sets of nPDFs [21–23]). In addition, these measurements may also help to probe, for the first time, the flavour dependence of nuclear modifications in quark

¹unless a deuterium target, complicated by possible nuclear corrections, is used.

densities [18]. The production of W bosons in heavy-ion collisions is also of paramount importance. Measurements by ATLAS [24] and CMS [25] in Pb–Pb collisions have revealed that the production rate approximately scales with the number of binary nucleon-nucleon collisions. This is in sharp contrast to hadronic observables (high-transverse momentum hadrons [26–28] and jets [29–31]) which are strongly suppressed as compared to p–p collisions. Thus, the leptons from W decays are valuable “messengers” from the initial state of heavy-ion collisions and could also be used to constrain the nPDFs [32–34].

In this paper, our main focus is on the centre-of-mass energy (\sqrt{s}) systematics of the production cross sections $d\sigma^{\ell^\pm}/dy$ in hadronic collisions and the consequent scaling properties of the lepton charge asymmetry. First, in Section 2, we show how the scaling laws for absolute cross sections and charge asymmetries emerge from the relatively simple leading-order expressions. In Section 3 we then contrast these expectations against next-to-leading order (NLO) computations. Section 4 presents comparisons with the existing world data from LHC and Tevatron experiments as well as our proposal for a precision observable that could be measured at the LHC. Finally, we summarize our main findings in Section 5.

2 Derivation of the scaling properties

2.1 Absolute cross sections

We consider the inclusive production of W bosons in high-energy collisions of two hadrons, H_1 and H_2 , followed by the decay of W to a charged lepton and a neutrino,

$$H_1 + H_2 \rightarrow W^- + X \rightarrow \ell^- + \bar{\nu} + X,$$

$$H_1 + H_2 \rightarrow W^+ + X \rightarrow \ell^+ + \nu + X.$$

At leading order, the production cross section double differential in the charged lepton rapidity y and transverse momentum p_T reads [35, 36],

$$\begin{aligned} \frac{d^2\sigma^{\ell^\pm}(s)}{dydp_T} &= \frac{\pi p_T}{24s^2} \left(\frac{\alpha_{\text{em}}}{\sin^2\theta_W} \right)^2 \sum_{i,j} \delta_{e_{q_i}+e_{\bar{q}_j}, \pm 1} |V_{ij}|^2 \times \\ &\int_{x_2^{\min}}^1 dx_2 \left(x_2 - \frac{p_T}{\sqrt{s}} e^{-y} \right)^{-1} \frac{(x_1 x_2)^{-1}}{(x_1 x_2 s - M_W^2)^2 + M_W^2 \Gamma_W^2} \times \\ &\left[(\hat{t} + \hat{u} \pm \hat{t} \mp \hat{u})^2 q_i^{\text{H}_1}(x_1, Q^2) \bar{q}_j^{\text{H}_2}(x_2, Q^2) + (\hat{t} + \hat{u} \mp \hat{t} \pm \hat{u})^2 \bar{q}_j^{\text{H}_1}(x_1, Q^2) q_i^{\text{H}_2}(x_2, Q^2) \right], \end{aligned} \quad (2.1)$$

where the symbols α_{em} , θ_W , and V_{ij} refer to the fine-structure constant, weak-mixing angle, and elements of Cabibbo-Kobayashi-Maskawa matrix, respectively. The mass and width of the W boson are denoted by M_W and Γ_W . The lower limit of the x_2 integral is given by $x_2^{\min} = (p_T e^{-y})/(\sqrt{s} - p_T e^y)$ and the momentum argument x_1 and the Mandelstam variables \hat{t} and \hat{u} are

$$x_1 = \frac{x_2 p_T e^y}{x_2 \sqrt{s} - p_T e^{-y}}, \quad \hat{t} = -\sqrt{s} p_T x_1 e^{-y}, \quad \hat{u} = -\sqrt{s} p_T x_2 e^y. \quad (2.2)$$

The PDFs are denoted by $q_i^{\text{H}^k}(x, Q^2)$ (with $Q^2 = \mathcal{O}(M_W^2)$) and the sum runs over all flavours i, j such that the electric charges e_{q_i} of the quarks sum up to ± 1 . Since the total width of the W boson is much smaller than its mass, $\Gamma_W \ll M_W$, we can make use of a delta-function identity $\epsilon/(x^2 + \epsilon^2) \rightarrow \pi\delta(x)$, as $\epsilon \rightarrow 0$, to perform the remaining integral in Eq. (2.1). We find

$$\begin{aligned} \frac{d^2\sigma^{\ell^\pm}(s)}{dydp_T} &\approx \frac{\pi^2}{24s} \left(\frac{\alpha_{\text{em}}}{\sin^2\theta_W} \right)^2 \frac{1}{M_W\Gamma_W} \frac{p_T}{\sqrt{1 - 4p_T^2/M_W^2}} \sum_{i,j} |V_{ij}|^2 \delta_{e_{q_i}+e_{\bar{q}_j}, \pm 1} \\ &\left\{ \left[1 \mp \sqrt{1 - 4p_T^2/M_W^2} \right]^2 q_i^{\text{H}_1}(x_1^+) \bar{q}_j^{\text{H}_2}(x_2^+) + \left[1 \pm \sqrt{1 - 4p_T^2/M_W^2} \right]^2 q_i^{\text{H}_1}(x_1^-) \bar{q}_j^{\text{H}_2}(x_2^-) + \right. \\ &\left. \left[1 \pm \sqrt{1 - 4p_T^2/M_W^2} \right]^2 \bar{q}_j^{\text{H}_1}(x_1^+) q_i^{\text{H}_2}(x_2^+) + \left[1 \mp \sqrt{1 - 4p_T^2/M_W^2} \right]^2 \bar{q}_j^{\text{H}_1}(x_1^-) q_i^{\text{H}_2}(x_2^-) \right\}, \end{aligned} \quad (2.3)$$

where the momentum arguments of the PDFs are

$$x_1^\pm \equiv \frac{M_W^2 e^y}{2p_T \sqrt{s}} \left[1 \mp \sqrt{1 - 4p_T^2/M_W^2} \right], \quad x_2^\pm \equiv \frac{M_W^2 e^{-y}}{2p_T \sqrt{s}} \left[1 \pm \sqrt{1 - 4p_T^2/M_W^2} \right]. \quad (2.4)$$

Let us first consider a situation with² $y \gg 0$, that is, $x_2^\pm < x_1^\pm$. In terms of a dimensionless variable ξ_1 (which coincides with x_1^\pm when $p_T \rightarrow M_W/2$),

$$\xi_1 \equiv \frac{M_W}{\sqrt{s}} e^y, \quad (2.5)$$

the momentum fractions in Eq. (2.4) become

$$x_1^\pm \equiv \frac{M_W}{2p_T} \xi_1 \left[1 \mp \sqrt{1 - 4p_T^2/M_W^2} \right], \quad x_2^\pm \equiv \frac{M_W^3}{2p_T s \xi_1} \left[1 \pm \sqrt{1 - 4p_T^2/M_W^2} \right]. \quad (2.6)$$

At sufficiently small x , the sea-quark densities at high $Q^2 \sim M_W^2$ should be reasonably well approximated by a power law [42]

$$x \bar{q}_i(x, Q^2) \approx x q_i(x, Q^2) \approx N_i x^{-\alpha}, \alpha > 0, \quad (2.7)$$

where the exponent α and the normalizations N_i should be almost flavour independent. Such a behaviour (though not exactly a power law) is expected by considering the small- x and large Q^2 limit (the so-called double logarithmic approximation [37]) of Dokshitzer-Gribov-Lipatov-Altarelli-Parisi parton evolution equations [38–41]. By using the approximation Eq. (2.7) in Eq. (2.3) and trading the rapidity variable y with ξ_1 , we find

$$\frac{d^2\sigma^{\ell^\pm}(s, \xi_1)}{dp_T d\xi_1} \approx s^\alpha \times f^\pm(\xi_1, p_T, H_1, H_2), \quad y \gg 0, \quad (2.8)$$

where $f^\pm(\xi, p_T, H_1, H_2)$ is a function that does not depend explicitly on s or y . Since the expression of Eq. (2.3) is peaked at $p_T \approx M_W/2$ and the p_T dependence of the probed

²For simplicity, $y \gg 0$ ($y \ll 0$) should be understood as $e^y \gg 1$ ($e^y \ll 1$) in the remainder of the paper.

momentum fractions in Eqs. (2.4) is not particularly fierce, the x interval spanned by integration over p_T with a typical experimental cut $p_T \gtrsim 20 \text{ GeV}$ should not be overly wide such that approximation of Eq. (2.7) remains valid. Under these conditions, the scaling law in Eq.(2.8) holds also for p_T -integrated cross sections,

$$\frac{d\sigma^{\ell^\pm}(s, \xi_1)}{d\xi_1} \approx s^\alpha \times F^\pm(\xi_1, H_1, H_2), \quad y \gg 0, \quad (2.9)$$

where $F^\pm(\xi_1, H_1, H_2) \equiv \int dp_T f^\pm(\xi_1, p_T, H_1) \theta(p_T - p_T^{\min})$. In the backward direction with $y \ll 0$, the appropriate scaling variable is

$$\xi_2 \equiv \frac{M_W}{\sqrt{s}} e^{-y}, \quad (2.10)$$

such that

$$\frac{d\sigma^{\ell^\pm}(s, \xi_2)}{d\xi_2} \approx s^\alpha \times G^\pm(\xi_2, H_1, H_2), \quad y \ll 0, \quad (2.11)$$

where $G^\pm(\xi_2, H_1, H_2)$ is a function that does not depend explicitly on s or y . If $H_1 = H_2$, then $F^\pm(\xi_1, H_1, H_2) = G^\pm(\xi_2, H_1, H_2)$.

2.2 Charge asymmetries

Since the \sqrt{s} dependence in Eqs. (2.9) and (2.11) is completely in the common prefactor s^α , it follows that the lepton charge asymmetry Eq. (1.1) should obey a particularly simple scaling law,

$$\begin{aligned} \mathcal{C}_\ell^{H_1, H_2}(s, \xi_1) &\approx F(\xi_1, H_1, H_2), \quad y \gg 0, \\ \mathcal{C}_\ell^{H_1, H_2}(s, \xi_2) &\approx G(\xi_2, H_1, H_2), \quad y \ll 0, \end{aligned} \quad (2.12)$$

where $F(\xi, H_1, H_2) \equiv (F^+(\xi, H_1, H_2) - F^-(\xi, H_1, H_2)) / (F^+(\xi, H_1, H_2) + F^-(\xi, H_1, H_2))$, and similarly for G . In other words, at fixed ξ_1 or ξ_2 , the charge-asymmetry should be approximately independent of the centre-of-mass energy. Another, and also a bit surprising feature of the charge asymmetry is that at large $|y|$ it effectively depends only on the nucleon that is probed at large x . This follows from the facts that when $|y|$ is sufficiently large, either $u\bar{d}$ or $d\bar{u}$ partonic process eventually dominates, and that the light-sea-quark distributions are expected to be approximately SU(2) symmetric at small x ,

$$u(x, Q^2) \approx \bar{u}(x, Q^2) \approx d(x, Q^2) \approx \bar{d}(x, Q^2), \quad x \ll 1, \quad (2.13)$$

and thus symmetric with respect to charge conjugation and isospin rotation. For example, one would expect that $\mathcal{C}_\ell^{\text{p,p}}(s, \xi_1) \approx \mathcal{C}_\ell^{\text{p},\bar{\text{p}}}(s, \xi_1)$ at large ξ_1 . In the case of nuclei the nPDFs $f_i^A(x, Q^2)$ are built from the free nucleon PDFs $f_i^{\text{proton}}(x, Q^2)$ and nuclear modification factors $R_i^{\text{proton}, A}$ by (see e.g. [20])

$$f_i^A(x, Q^2) = Z f_i^{\text{proton}, A}(x, Q^2) + N f_i^{\text{neutron}, A}(x, Q^2), \quad (2.14)$$

where

$$f_i^{\text{proton}, A}(x, Q^2) = R_i^{\text{proton}, A} f_i^{\text{proton}}(x, Q^2), \quad (2.15)$$

$$f_i^{\text{neutron}, A}(x, Q^2) = f_{i, u \leftrightarrow d}^{\text{proton}, A}(x, Q^2). \quad (2.16)$$

At small- x one expects modest shadowing ($R_i^{\text{proton},A} < 1$) which, however, should not significantly alter the scaling exponent α (particularly at high $Q^2 \sim M_W^2$ involved here) and, to a good approximation, the effect of shadowing is just a slight overall downward normalization in the absolute cross sections which should largely disappear in the case of charge asymmetry. In other words, we can encapsulate the scaling law for lepton charge asymmetry as

$$\begin{aligned} \mathcal{C}_\ell^{\text{H}_1, \text{H}_2}(s, \xi_1) &\approx F(\xi_1, \text{H}_1), & y \gg 0, \\ \mathcal{C}_\ell^{\text{H}_1, \text{H}_2}(s, \xi_2) &\approx G(\xi_2, \text{H}_2), & y \ll 0, \end{aligned} \quad (2.17)$$

independently of the nature of hadron (nucleon, anti-nucleon, nucleus) probed at small x .

3 Scaling vs. NLO calculation

Most of our plots in the rest of the paper will use the scaling variables $\xi_{1,2}$ which are related to rapidity y and centre-of-mass energy \sqrt{s} via Eq. (2.5) and Eq. (2.10). To ease the interpretation in what follows, this dependence is illustrated in Figure 1.

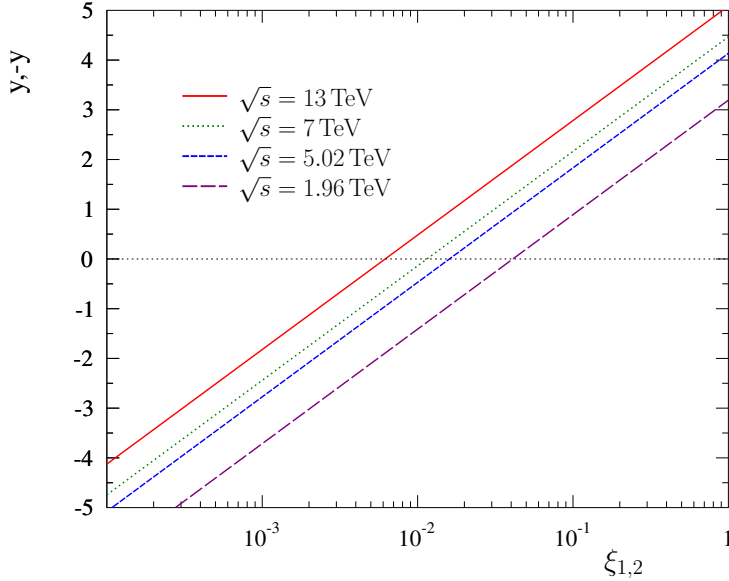


Figure 1. Relation of rapidity y and scaling variables $\xi_{1,2}$ for a few values of \sqrt{s} .

According to Eq. (2.7), the scaling exponent α in Eq. (2.9) should reflect the small- x behaviour of quark distributions and it can be straightforwardly extracted from cross-sections at two different centre-of-mass energies. To verify this correspondence and the consistency of our derivation, we have computed the full NLO cross-sections at $\sqrt{s} = 7, 8, 13$ TeV for p-p collisions using MCFM Monte-Carlo code [45] and CT10NLO PDFs [17].

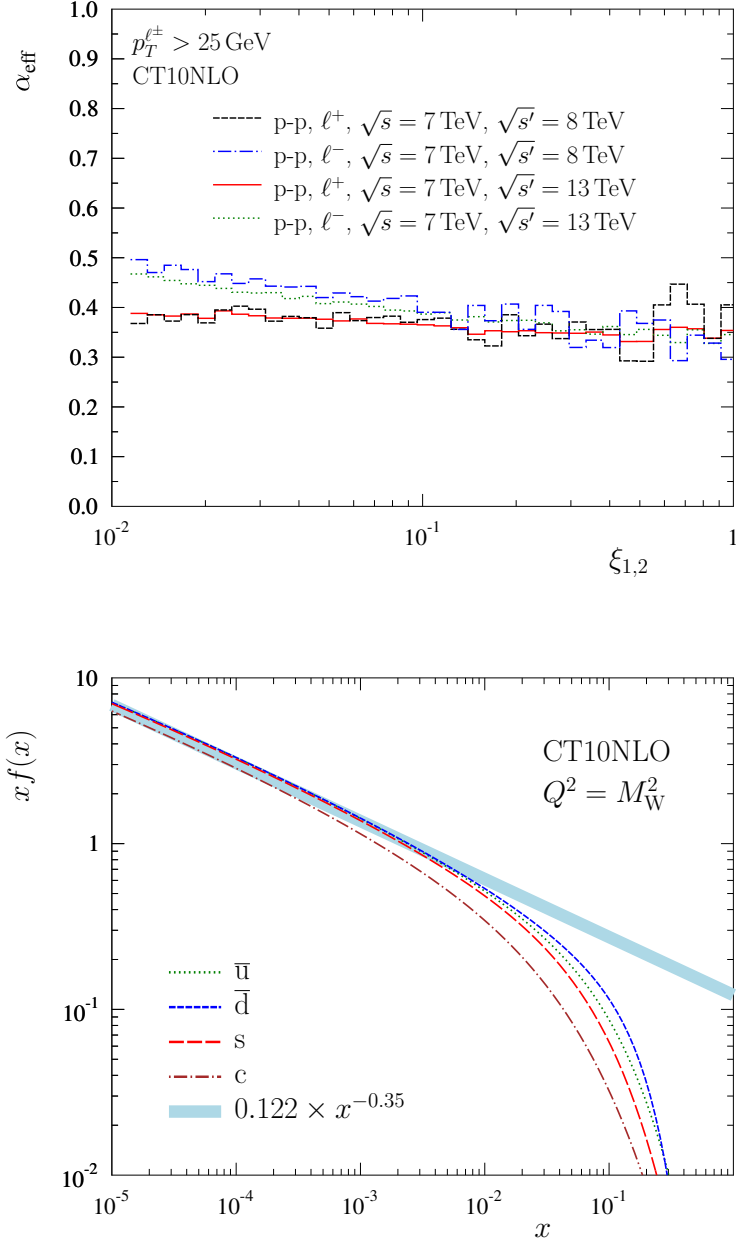


Figure 2. Scaling exponent extracted from NLO calculations (upper panel) and its comparison with CT10NLO PDFs (lower panel).

From these cross-sections, we have evaluated the effective scaling exponent α_{eff} by

$$\alpha_{\text{eff}}(\xi) = \log \left[\frac{\sigma^{\ell^\pm}(s, \xi)/d\xi}{\sigma^{\ell^\pm}(s', \xi)/d\xi} \right] \log^{-1} \left(\frac{s}{s'} \right), \quad (3.1)$$

taking $\sqrt{s} = 7 \text{ TeV}$ and $\sqrt{s'} = 8, 13 \text{ TeV}$. The outcome is plotted in the upper panel

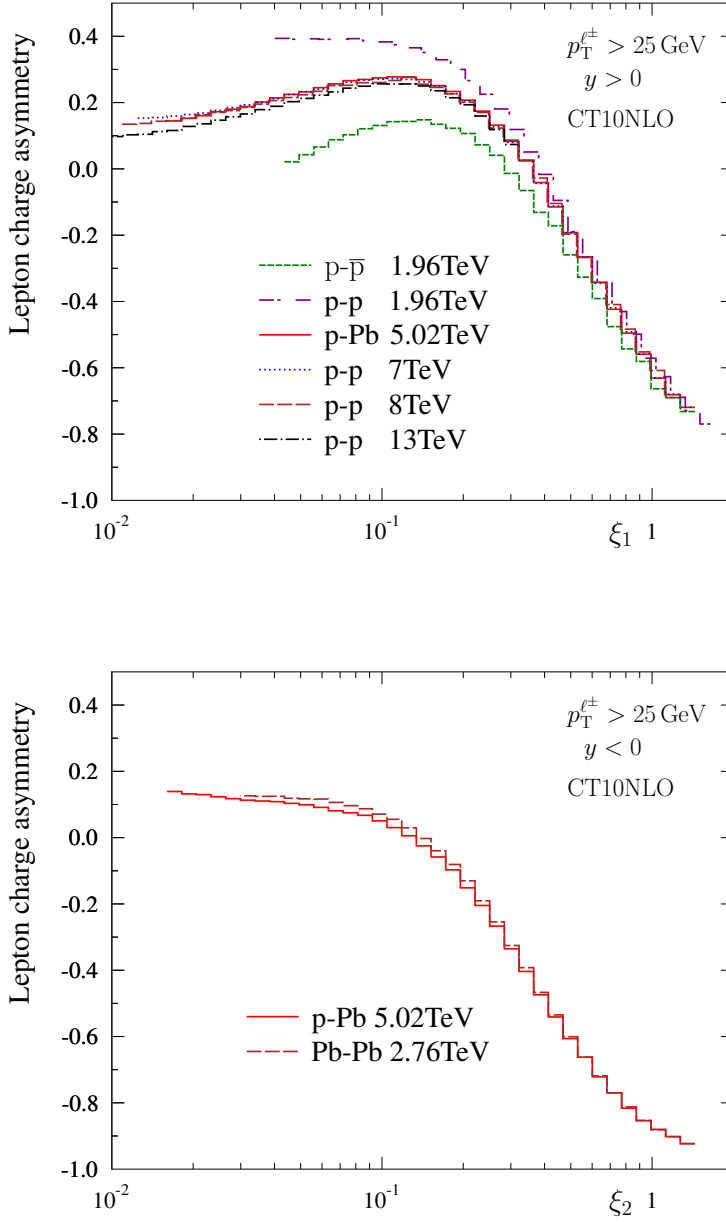


Figure 3. Lepton charge asymmetry in $p\bar{p}$ ($\sqrt{s} = 1.96$ TeV), $p\text{-}p$ ($\sqrt{s} = 1.96, 7, 8$ TeV), $p\text{-}Pb$ ($\sqrt{s} = 5.02$ TeV) and $Pb\text{-}Pb$ ($\sqrt{s} = 2.76$ TeV) collisions, for $y > 0$ (upper panel) and $y < 0$ (lower panel).

of Figure 2. To first approximation, towards large $\xi_{1,2}$ the effective scaling exponent is $\alpha_{\text{eff}} \approx 0.35$ and independent of the lepton charge. In more detail, the scaling exponent is not exactly constant but some variation is visible which reflects the fact that the PDFs do not follow a pure power law, especially when x is not very small (at small $\xi_{1,2}$). The

scaling exponent for ℓ^- tends to have more slope and to be somewhat larger than that of ℓ^+ especially at small $\xi_{1,2}$ which corresponds to midrapidity. This can be explained by the slightly steeper slope of the \bar{u} distribution in comparison to \bar{d} distribution (see the lower panel of Figure 2) and the fact that ℓ^- production tends to be sensitive to somewhat larger values of x in the small- x side. The latter follows from the factors $(1 \pm \sqrt{1 - 4p_T^2/M_W^2})^2$ that multiply PDFs in Eq. (2.3). These, in turn, originate from the parity non-conserving W couplings to quarks and leptons. The lower panel in Figure 2 compares the extracted exponent $\alpha_{\text{eff}} \approx 0.35$ to the CT10NLO sea-quark PDFs. Evidently, there is a good correspondence between the scaling exponent α and the behaviour of the small- x quark PDFs. We can conclude that despite the complex higher-order QCD calculations, the centre-of-mass dependence of the cross sections being discussed can be essentially captured by a simple power law.

Let us now discuss Eq. (2.17) and whether the nature of the hadronic projectile or nucleus probed at small x really disappears as conjectured. To this end we have computed the lepton charge asymmetry (again, at NLO accuracy) in various collision systems at centre-of-mass energies that correspond to existing Tevatron and LHC data. The results are shown in Figure 3. At $y \gg 0$, the curves corresponding to p-p, p-Pb and p- \bar{p} tend to unite, whereas in the opposite direction, $y \ll 0$, p-Pb and Pb-Pb become approximately the same. Thus, as far as theoretical NLO expectations are concerned, the scaling law of Eq. (2.17) turns out to be a very good approximation, though not perfect. The largest deviations in Figure 3 are seen in the case of p- \bar{p} at the Tevatron energy, $\sqrt{s} = 1.96$ TeV. There, the probed values of x for \bar{p} are not small enough and especially the assumption of charge-conjugation symmetric quark distributions, Eq. (2.13), is not particularly accurate until almost the end of phase space (e.g. $\xi_1 = 1$ corresponds to $x_2 \approx M_W^2/s \approx 0.002$). The p-p curve at the same center-of-mass energy unites with the rest already at lower ξ_1 .

At small fixed value of ξ , the lepton charge asymmetry in p-p collisions tends to decrease towards increasing centre-of-mass energies. This can be interpreted in terms of slightly different scaling exponent for ℓ^+ and ℓ^- production (see Figure 2). Denoting the scaling exponent for ℓ^\pm production by α^\pm , and the difference by $\Delta \equiv \alpha^- - \alpha^+$, to first approximation,

$$\mathcal{C}_\ell^{\text{H}_1, \text{H}_2}(s', \xi) = \mathcal{C}_\ell^{\text{H}_1, \text{H}_2}(s, \xi) + \frac{\Delta}{2} \left\{ 1 - \left[\mathcal{C}_\ell^{\text{H}_1, \text{H}_2}(s, \xi) \right]^2 \right\} \log \left(\frac{s}{s'} \right) + \mathcal{O}(\Delta^2). \quad (3.2)$$

Since $\Delta > 0$, we have a condition

$$\mathcal{C}_\ell^{\text{H}_1, \text{H}_2}(s', \xi) < \mathcal{C}_\ell^{\text{H}_1, \text{H}_2}(s, \xi), \text{ if } s' > s, \quad (3.3)$$

which explains the decreasing trend of lepton charge asymmetries in p-p collisions towards higher centre-of-mass energies at fixed, small ξ .

4 Data and predictions

4.1 Comparison with existing data

The currently most accurate experimental measurements for inclusive W production from Tevatron and LHC experiments are summarized in Table 1. A direct comparison of vari-

Table 1. The experimental data sets.

Experiment	System	\sqrt{s}	kinematic cuts	Ref.
D0	p- \bar{p}	1.96 TeV	$p_T > 25 \text{ GeV}, \cancel{E}_T > 25 \text{ GeV}$	[8]
ATLAS	Pb-Pb	2.76 TeV	$p_T > 25 \text{ GeV}, \cancel{E}_T > 25 \text{ GeV}, m_T > 40 \text{ GeV}$	[24]
CMS	p-Pb	5.02 TeV	$p_T > 25 \text{ GeV}$	[18]
ALICE	p-Pb	5.02 TeV	$p_T > 10 \text{ GeV}$	[19]
CMS	p-p	7 TeV	$p_T > 25 \text{ GeV}$	[11]
ATLAS	p-p	7 TeV	$p_T > 20 \text{ GeV}, \cancel{E}_T > 25 \text{ GeV}, m_T > 40 \text{ GeV}$	[46]
LHCb	p-p	7 TeV	$p_T > 20 \text{ GeV}$	[13]
CMS	p-p	8 TeV	$p_T > 25 \text{ GeV}$	[12]

ous measurements is complicated by the kinematic cuts for lepton p_T , missing transverse energy \cancel{E}_T , and transverse mass m_T of the neutrino-lepton system, which vary among the experiments and have to be accounted for. Here, we have chosen to “correct” the data to $p_T > 25 \text{ GeV}$ (the default cut in CMS measurements) by MCFM evaluating the observables first with the true cuts shown in Table 1, then with $p_T > 25 \text{ GeV}$ and taking the ratio (absolute cross sections) or difference (charge asymmetry). We stress that if the kinematic cuts were the same in all experiments, this step would be unnecessary. The available absolute cross sections are compared in Figure 4 at forward rapidity (p-p and p-Pb collisions) and in Figure 5 at backward rapidity (Pb-Pb and p-Pb collisions) scaled by a factor $(s/\text{GeV}^2)^{-\alpha}$. A constant value $\alpha = 0.4$ has been used for the scaling exponent as a compromise between the expected exponent at small and large ξ , see Figure 2. Keeping in mind the “non-constantness” of the scaling exponent and that at forward (backward) direction the p-Pb (Pb-Pb) data are presumably affected by small- x shadowing ($\sim 10\%$ suppression according to the current nPDFs) in comparison to p-p (p-Pb), an exact match with p-p (p-Pb) is not expected. Nevertheless, there is clearly a rough correspondence between the data from different collision systems.

The data for lepton charge asymmetries \mathcal{C}_ℓ are compiled in Figure 6. We note that some experimental uncertainties, luminosity above all, cancel in the measurement of the lepton charge asymmetries as compared to absolute cross sections. As previously, the data from p-p, p- \bar{p} , and Pb-Pb collisions are plotted only in the direction where they are supposed to merge with p-Pb data. To a very good approximation, the experimental data indeed line up to the same underlying curve which corresponds to the charge asymmetry in p-Pb collisions. This confirms that our simple scaling law of Eq. (2.17) is an excellent approximation. We can also compress all the data into a single plot. This is done by choosing a certain reference centre-of-mass energy $\sqrt{s_{\text{ref}}}$ (we take $\sqrt{s_{\text{ref}}} = 5.02 \text{ TeV}$) and plotting the data as a function of variable

$$y_{\text{ref}} \equiv y \pm \frac{1}{2} \log \frac{s_{\text{ref}}}{s}, \quad y \gtrless 0, \quad (4.1)$$

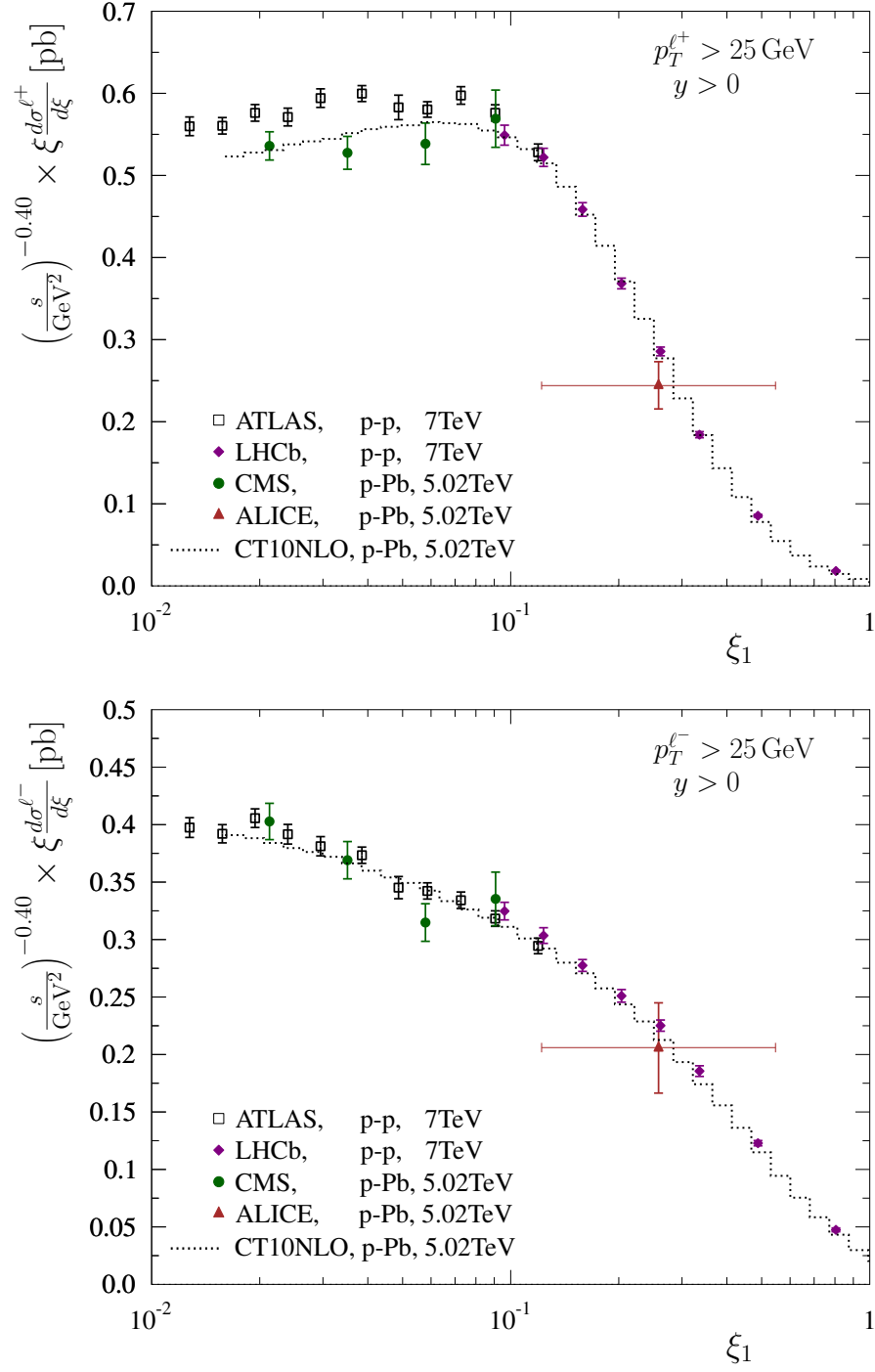


Figure 4. Absolute spectra of charged leptons (upper panel for ℓ^+ , lower panel for ℓ^-) in p-p ($\sqrt{s} = 7$ TeV) and p-Pb ($\sqrt{s} = 5.02$ TeV) collisions for $y > 0$, scaled by $(s/\text{GeV}^2)^{-0.40}$.

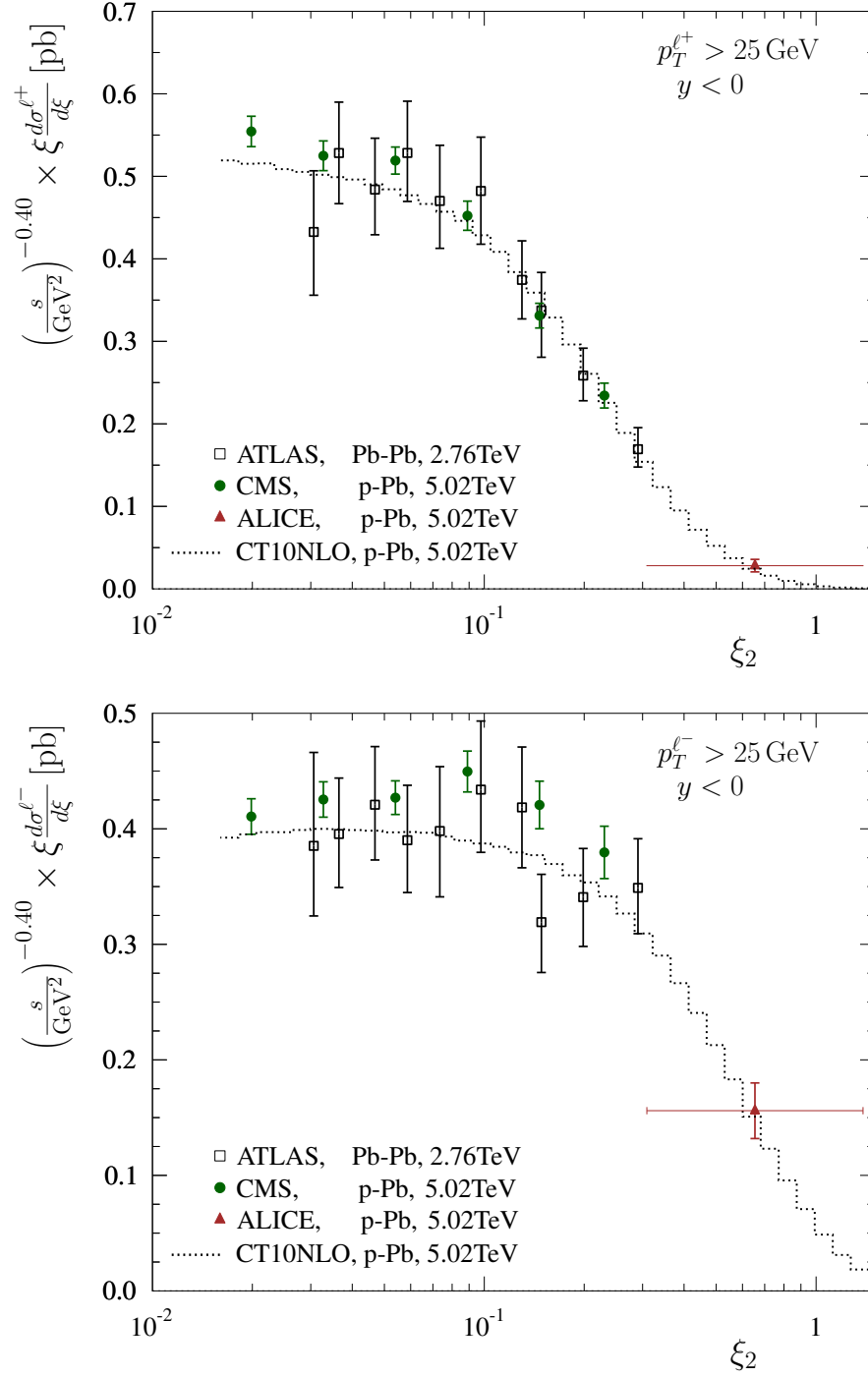


Figure 5. Absolute spectra of charged leptons (upper panel for ℓ^+ , lower panel for ℓ^-) in Pb-Pb ($\sqrt{s} = 2.76$ TeV) and p-Pb ($\sqrt{s} = 5.02$ TeV) collisions for $y > 0$, scaled by $(s/\text{GeV}^2)^{-0.40}$.

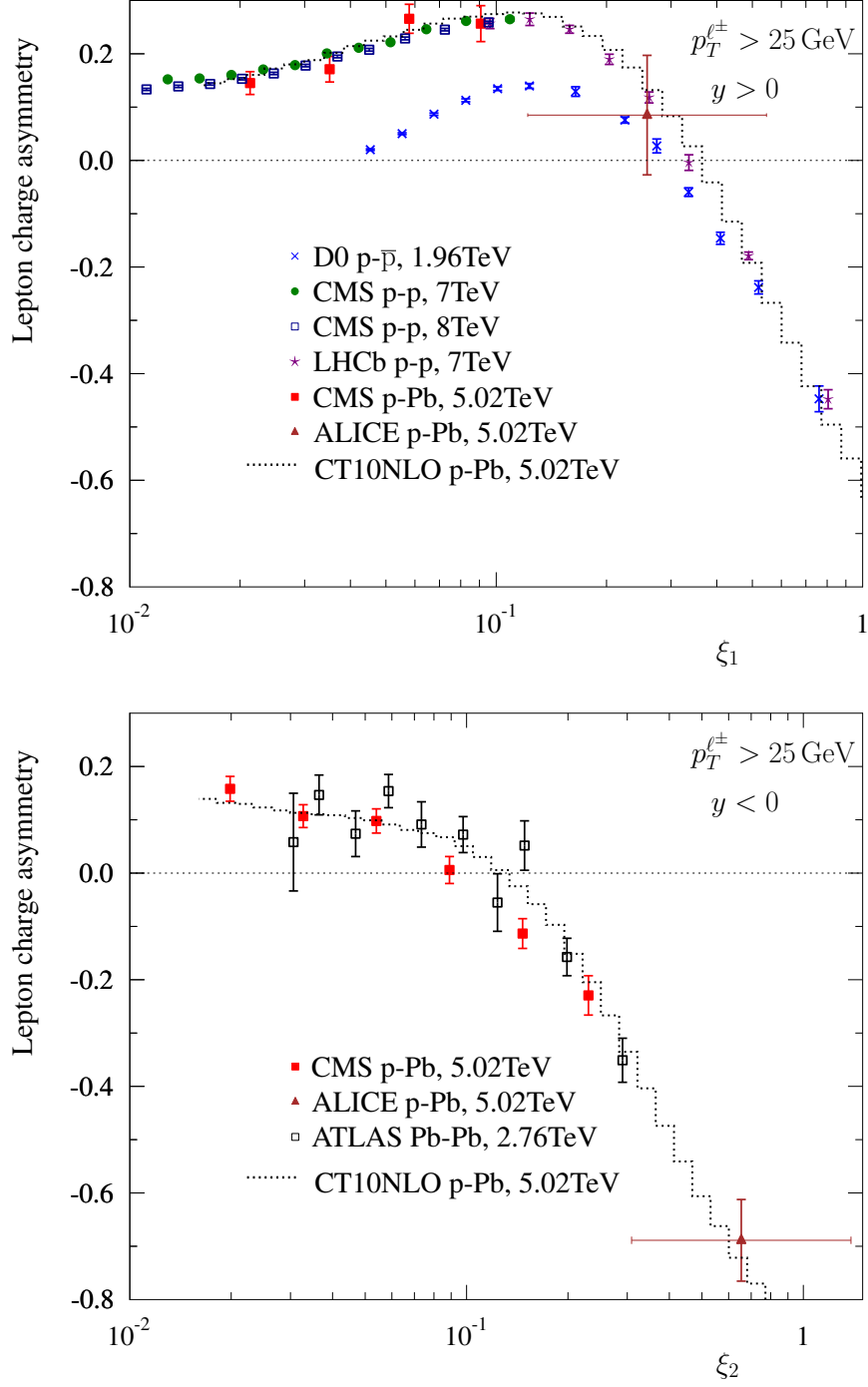


Figure 6. Lepton charge asymmetry in p- \bar{p} ($\sqrt{s} = 1.96$ TeV), p-p ($\sqrt{s} = 7, 8$ TeV), p-Pb ($\sqrt{s} = 5.02$ TeV) and Pb-Pb ($\sqrt{s} = 2.76$ TeV) collisions. The dotted curve is to guide the eye and corresponds to $C_\ell^{\text{p,Pb}}$ at $\sqrt{s} = 5.02$ TeV.

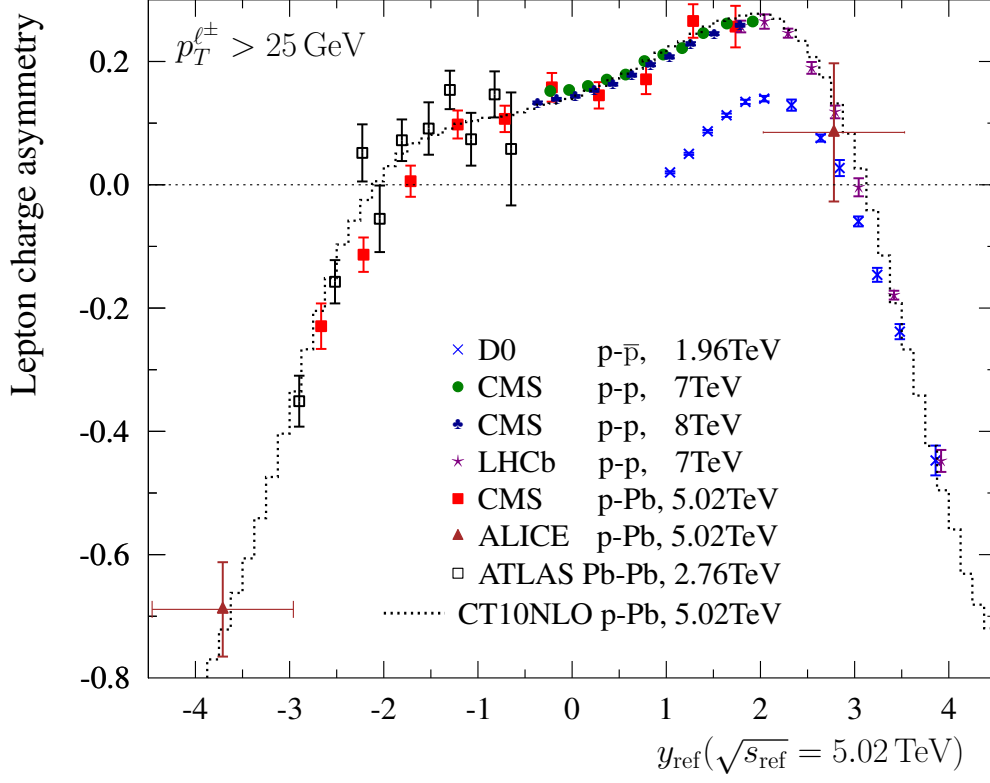


Figure 7. The world data on lepton charge asymmetry as a function of y_{ref} taking $\sqrt{s_{\text{ref}}} = 5.02$ TeV.

such that

$$\begin{aligned}\xi_1(y, \sqrt{s}) &= \xi_1(y_{\text{ref}}, \sqrt{s_{\text{ref}}}), & y > 0, \\ \xi_2(y, \sqrt{s}) &= \xi_2(y_{\text{ref}}, \sqrt{s_{\text{ref}}}), & y < 0.\end{aligned}\tag{4.2}$$

Such a plot is shown in Figure 7. In order to keep the plot readable Pb-Pb data is plotted only at $y < 0$, and p-p, p- \bar{p} data is plotted only at $y > 0$.

4.2 Predictions

Having now verified that the bulk part of the behaviour of charge asymmetries at $|y| \gg 0$ can be accounted for by a simple scaling law, we can also take advantage of this to make accurate predictions. On one hand, given a data point at a certain centre-of-mass energy \sqrt{s} and rapidity y , we can compute a prediction for another centre-of-mass energy $\sqrt{s'}$ at shifted rapidity $y' = y \pm 0.5 \log(s'/s)$ (so that either scaling variable ξ_1 in Eq. (2.5) or ξ_2 in Eq. (2.10) stays constant) by

$$\mathcal{C}_\ell(s', y \pm \frac{1}{2} \log(s'/s)) = \frac{[1 + \mathcal{C}_\ell(s, y)] \mathcal{D} - [1 - \mathcal{C}_\ell(s, y)]}{[1 + \mathcal{C}_\ell(s, y)] \mathcal{D} + [1 - \mathcal{C}_\ell(s, y)]},\tag{4.3}$$

where

$$\mathcal{D} \equiv \left[\frac{d\sigma^{\ell^+}(y', s')/dy'}{d\sigma^{\ell^-}(y', s')/dy'} \right] \left[\frac{d\sigma^{\ell^+}(y, s)/dy}{d\sigma^{\ell^-}(y, s)/dy} \right]^{-1}, \quad (4.4)$$

is a PDF-dependent factor that estimates the corrections for the residual effects that Eq. (2.17) does not account for (the different scaling exponent α for ℓ^+ and ℓ^- , see Figure 2). On the other hand, the double ratio \mathcal{D} is itself an observable that can be predicted with a high accuracy. Both cases are illustrated below.

Predictions for the charge asymmetry in 8 TeV p-p collisions, based on 7 TeV p-p measurements, are shown in Figure 8 and compared to an ordinary prediction using CT10NLO PDFs. The existing CMS data at 8 TeV [12] are also shown. Most of the uncertainty in our prediction comes from the experimental uncertainty of the 7 TeV measurements and the uncertainties in CT10NLO PDFs that feed into our prediction via correction factors \mathcal{D} are always smaller than the experimental uncertainties. The drawback of this procedure is that there is no flexibility in choosing the rapidity bins of the predictions, but they are tied to the existing data and to the difference in the two centre-of-mass energies. This e.g. hinders the quantitative comparison with the CMS 8 TeV data unless further assumptions are made (which would partly undermine the accuracy achieved by the scaling).

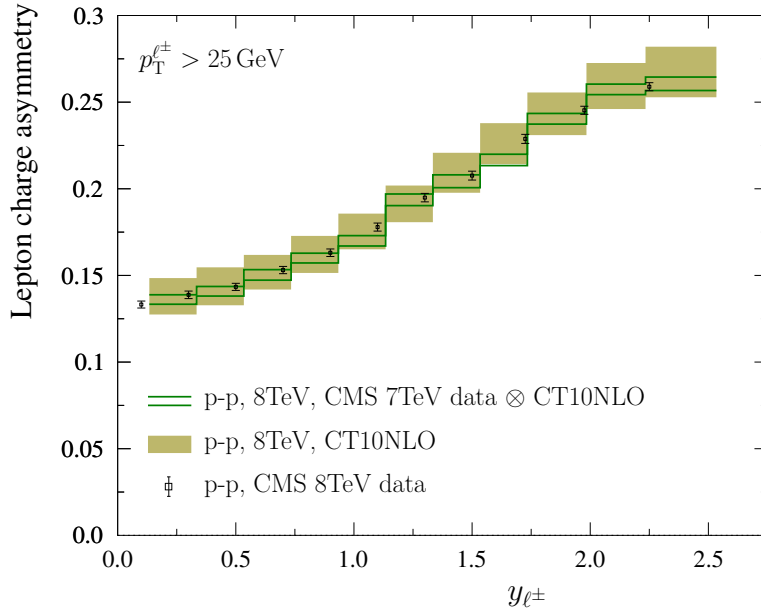


Figure 8. Lepton charge asymmetries in 8 TeV p-p collisions. The yellow filled boxes correspond to a direct computation with CT10NLO PDFs and the green rectangles show the predictions based on the CMS 7 TeV data as described in the text. The measurements of CMS [12] are also shown.

In Figure 9 we show the double ratio \mathcal{D} in p-p collisions as a function of ξ_1 computed with CT10NLO PDFs in two different cases: $(\sqrt{s'}, \sqrt{s}) = (8 \text{ TeV}, 7 \text{ TeV})$ and $(\sqrt{s'}, \sqrt{s}) = (14 \text{ TeV}, 13 \text{ TeV})$. For comparison, the central predictions of MMHT PDFs [47] are shown

as well. In both cases the results remain close to unity with very small PDF uncertainty. Towards large ξ_1 the spread between CT10NLO and MMHT results gets small which was to be expected as at large values of ξ_1 the scaling relations become increasingly accurate and the predictions are less sensitive to the input PDFs.³ Thus, measurement of the double ratio at the LHC would constitute a precision test of the perturbative QCD and electro-weak theory.

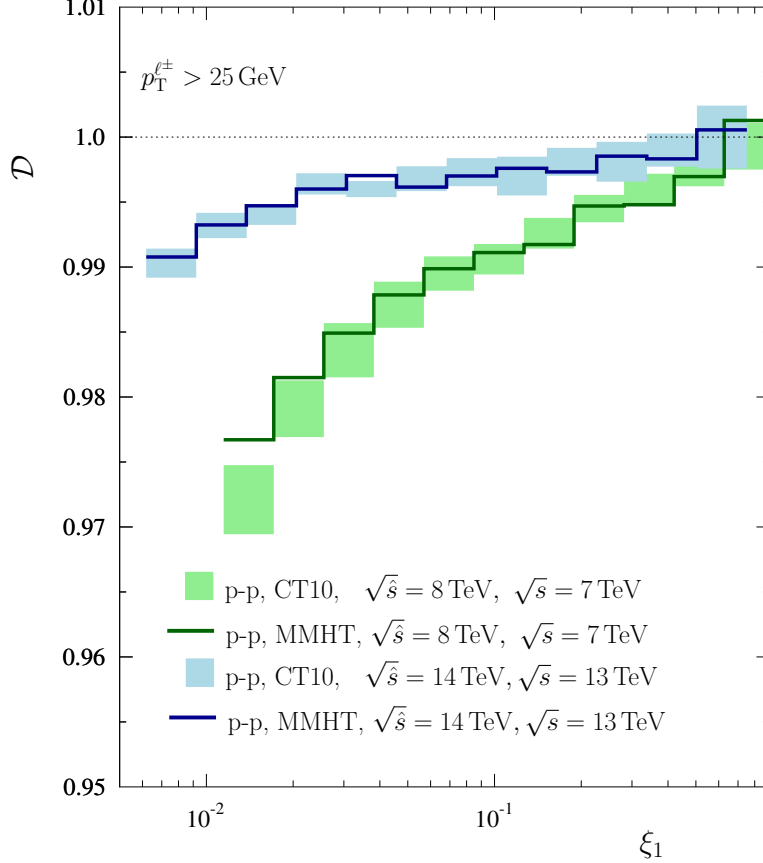


Figure 9. The double ratio \mathcal{D} computed with CT10NLO (coloured rectangles) and MMHT (lines) for $\sqrt{s'} = 8$ TeV, $\sqrt{s} = 7$ TeV (green) and $\sqrt{s'} = 14$ TeV, $\sqrt{s} = 13$ TeV (blue).

5 Summary

We have discussed the scaling properties of inclusive charged leptons from decays of W bosons created in hadronic collisions. Based on the leading-order estimate, we have found that the \sqrt{s} dependence of cross sections in forward/backward directions at fixed value of scaling variable $\xi_{1,2} = (M_W/\sqrt{s})e^{\pm y}$ should approximately obey a one-parameter power law, in which the scaling exponent is approximately independent of the lepton charge

³Even a better precision can be attained by considering the ratios of *total* cross sections [48] which, however, are more difficult to measure for the finite acceptance of the experimental apparatuses.

and reflects the slope of the small- x PDFs. Consequently, the lepton charge asymmetries at different centre-of-mass energies are predicted to be approximately same at fixed $\xi_{1,2}$. Moreover, lepton charge asymmetries in different collision systems are related: at large positive (negative) y the lepton charge asymmetry depends effectively only on the nature of the forward- (backward-) going nucleon or nucleus. A comparison with the experimental data from LHC and Tevatron confirms that the derived scaling laws are indeed able to capture very well the behaviour of the data. A dedicated experimental determination of W cross-section and charge asymmetries as a function of scaling variables $\xi_{1,2}$ at two different centre-of-mass energies is thus proposed as a precision test of the perturbative methods in collider physics.

Acknowledgments

We would like to thank Raphaël Granier de Cassagnac for discussions. We acknowledge CSC (IT Center for Science in Espoo, Finland) for computational resources. The work of ÉC is supported by the European Research Council, under the “QuarkGluonPlasmaCMS” #259612 grant.

References

- [1] E. L. Berger, F. Halzen, C. S. Kim and S. Willenbrock, Phys. Rev. D **40** (1989) 83 [Phys. Rev. D **40** (1989) 3789].
- [2] A. D. Martin, R. G. Roberts and W. J. Stirling, Mod. Phys. Lett. A **4** (1989) 1135.
- [3] F. Abe *et al.* [CDF Collaboration], Phys. Rev. Lett. **81** (1998) 5754 [hep-ex/9809001].
- [4] D. Acosta *et al.* [CDF Collaboration], Phys. Rev. D **71** (2005) 051104 [hep-ex/0501023].
- [5] V. M. Abazov *et al.* [D0 Collaboration], Phys. Rev. Lett. **101** (2008) 211801 [arXiv:0807.3367 [hep-ex]].
- [6] V. M. Abazov *et al.* [D0 Collaboration], Phys. Rev. D **77** (2008) 011106 [arXiv:0709.4254 [hep-ex]].
- [7] V. M. Abazov *et al.* [D0 Collaboration], Phys. Rev. D **88** (2013) 091102 [arXiv:1309.2591 [hep-ex]].
- [8] V. M. Abazov *et al.* [D0 Collaboration], Phys. Rev. D **91** (2015) 3, 032007 [arXiv:1412.2862 [hep-ex]].
- [9] G. Aad *et al.* [ATLAS Collaboration], JHEP **1012** (2010) 060 [arXiv:1010.2130 [hep-ex]].
- [10] G. Aad *et al.* [ATLAS Collaboration], Phys. Lett. B **701** (2011) 31 [arXiv:1103.2929 [hep-ex]].
- [11] S. Chatrchyan *et al.* [CMS Collaboration], Phys. Rev. D **90** (2014) 3, 032004 [arXiv:1312.6283 [hep-ex]].
- [12] CMS Collaboration [CMS Collaboration], CMS-PAS-SMP-14-022.
- [13] R. Aaij *et al.* [LHCb Collaboration], JHEP **1412** (2014) 079 [arXiv:1408.4354 [hep-ex]].
- [14] C. Anastasiou, L. J. Dixon, K. Melnikov and F. Petriello, Phys. Rev. D **69** (2004) 094008 [hep-ph/0312266].

- [15] S. Catani, L. Cieri, G. Ferrera, D. de Florian and M. Grazzini, Phys. Rev. Lett. **103** (2009) 082001 [arXiv:0903.2120 [hep-ph]].
- [16] R. D. Ball *et al.* [NNPDF Collaboration], Nucl. Phys. B **849** (2011) 112 [Nucl. Phys. B **854** (2012) 926] [Nucl. Phys. B **855** (2012) 927] [arXiv:1012.0836 [hep-ph]].
- [17] H. L. Lai, M. Guzzi, J. Huston, Z. Li, P. M. Nadolsky, J. Pumplin and C.-P. Yuan, Phys. Rev. D **82** (2010) 074024 [arXiv:1007.2241 [hep-ph]].
- [18] V. Khachatryan *et al.* [CMS Collaboration], arXiv:1503.05825 [nucl-ex].
- [19] J. Zhu [ALICE Collaboration], J. Phys. Conf. Ser. **612** (2015) 1, 012009.
- [20] K. J. Eskola, H. Paukkunen and C. A. Salgado, JHEP **0904** (2009) 065 [arXiv:0902.4154 [hep-ph]].
- [21] M. Hirai, S. Kumano and T.-H. Nagai, Phys. Rev. C **76** (2007) 065207 [arXiv:0709.3038 [hep-ph]].
- [22] K. Kovarik *et al.*, arXiv:1509.00792 [hep-ph].
- [23] D. de Florian, R. Sassot, P. Zurita and M. Stratmann, Phys. Rev. D **85** (2012) 074028 [arXiv:1112.6324 [hep-ph]].
- [24] G. Aad *et al.* [ATLAS Collaboration], Eur. Phys. J. C **75** (2015) 1, 23 [arXiv:1408.4674 [hep-ex]].
- [25] S. Chatrchyan *et al.* [CMS Collaboration], Phys. Lett. B **715** (2012) 66 [arXiv:1205.6334 [nucl-ex]].
- [26] S. Chatrchyan *et al.* [CMS Collaboration], Eur. Phys. J. C **72** (2012) 1945 [arXiv:1202.2554 [nucl-ex]].
- [27] G. Aad *et al.* [ATLAS Collaboration], arXiv:1504.04337 [hep-ex].
- [28] B. B. Abelev *et al.* [ALICE Collaboration], Phys. Lett. B **736** (2014) 196 [arXiv:1401.1250 [nucl-ex]].
- [29] CMS Collaboration [CMS Collaboration], CMS-PAS-HIN-12-004.
- [30] G. Aad *et al.* [ATLAS Collaboration], Phys. Rev. Lett. **114** (2015) 7, 072302 [arXiv:1411.2357 [hep-ex]].
- [31] J. Adam *et al.* [ALICE Collaboration], Phys. Lett. B **746** (2015) 1 [arXiv:1502.01689 [nucl-ex]].
- [32] H. Paukkunen and C. A. Salgado, JHEP **1103** (2011) 071 [arXiv:1010.5392 [hep-ph]].
- [33] P. Ru, B. W. Zhang, L. Cheng, E. Wang and W. N. Zhang, arXiv:1412.2930 [nucl-th].
- [34] P. Ru, B. W. Zhang, E. Wang and W. N. Zhang, arXiv:1505.08106 [nucl-th].
- [35] P. Aurenche and J. Lindfors, Nucl. Phys. B **185** (1981) 274.
- [36] H. Baer and M. H. Reno, Phys. Rev. D **43** (1991) 2892.
- [37] L.V. Gribov, E.M. Levin, M.G. Ryskin, Nucl. Phys. B **188** (1981) 555.
- [38] Y. L. Dokshitzer, Sov. Phys. JETP **46** (1977) 641 [Zh. Eksp. Teor. Fiz. **73** (1977) 1216].
- [39] V. N. Gribov and L. N. Lipatov, Sov. J. Nucl. Phys. **15** (1972) 438 [Yad. Fiz. **15** (1972) 781].
- [40] V. N. Gribov and L. N. Lipatov, Sov. J. Nucl. Phys. **15** (1972) 675 [Yad. Fiz. **15** (1972) 1218].
- [41] G. Altarelli and G. Parisi, Nucl. Phys. B **126** (1977) 298.

- [42] M. Gluck, E. Reya and A. Vogt, Eur. Phys. J. C **5** (1998) 461 [hep-ph/9806404].
- [43] A. Kusina, K. Kovaik, T. Jeo, D. B. Clark, F. I. Olness, I. Schienbein and J. Y. Yu, PoS DIS **2014** (2014) 047 [arXiv:1408.1114 [hep-ph]].
- [44] H. Paukkunen and C. A. Salgado, Phys. Rev. Lett. **110** (2013) 21, 212301 [arXiv:1302.2001 [hep-ph]].
- [45] J. M. Campbell and R. K. Ellis, Nucl. Phys. Proc. Suppl. **205-206** (2010) 10 [arXiv:1007.3492 [hep-ph]].
- [46] G. Aad *et al.* [ATLAS Collaboration], Phys. Rev. D **85** (2012) 072004 [arXiv:1109.5141 [hep-ex]].
- [47] L. A. Harland-Lang, A. D. Martin, P. Motylinski and R. S. Thorne, Eur. Phys. J. C **75** (2015) 5, 204 [arXiv:1412.3989 [hep-ph]].
- [48] M. L. Mangano and J. Rojo, JHEP **1208** (2012) 010 [arXiv:1206.3557 [hep-ph]].